

Engineering Behavior of Remolded Diatomaceous Silts

by

Talenta Pitso

A PROJECT

submitted to

Oregon State University

in partial fulfillment of
the requirements for the
degree of

Master of Science in Civil Engineering

Presented August 15, 2022

Commencement June 2022

ABSTRACT OF THE PROJECT OF

Talenta Pitso for the degree of Master of Science presented on August 15, 2022. Title: Evaluation of the Mechanical Behavior of Remolded Diatomaceous Silts.

Diatomaceous soils are a geological material whose engineering properties do not readily conform to the widely accepted and used mechanical and behavioral frameworks. This ambiguity results in design difficulties and geotechnical failures which can be costly. Diatomaceous soils have diatoms in their matrix. Diatoms are unicellular algae with an inert siliceous cell wall called a frustule. The rough surface area of the frustule contributes to diatomaceous soil's high shear strength. The frustule has high intraparticle porosity which increases the water affinity of diatomaceous soils. This study used Atterberg limit, lab vane, constant rate of strain, and direct simple shear tests to characterize the geotechnical properties of remolded diatomaceous silts. The results showed the diatomaceous silts to have high strength, high liquid limits, and high compressibility. The results of the remolded diatomaceous silts were compared to those of undisturbed specimens. Both the compressibility ratio and peak shear strength ($\sigma'_{vc} = 400kPa$) of remolded specimens were higher than of undisturbed specimens. The shear strength ratio and excess porewater generation of the two soil groups was similar at 25% strain.

Corresponding e-mail address: pitsot@oregonstate.edu

© Copyright by Talenta Pitso

August 15, 2022

ACKNOWLEDGEMENTS

I would like to express my sincerest appreciation and gratitude to my advisor, Dr. Matt Evans, for his endless encouragement and kindness. I would have not made it through the program without his direct and indirect support. Thank you for always making it feel like it is going to be okay. Thank you for your patience and believing in me. I will make you proud!

To Jiayao Wang, who showed me the ropes on everything to do with this project, thank you for your assistance and guidance. You made it look easy.

I would also like to thank my committee members for their input on improvements that can be made on the work presented. I am thankful to my family, friends and classmates for being my escapes when it got tough and laugh buddies when it was not so tough.

Lastly, my gratitude goes to Fulbright Scholarship for affording me the opportunity to pursue my master's degree. I now get to call myself a Fulbright alumni!

Contents

List of Figures	iii
List of Tables	v
1. Introduction.....	1
1.1 Background	1
2.1 Research objectives and goals.....	2
2. Review of Previous Studies	4
2.1 Atterberg Limits	5
2.2 Shear Strength	7
2.3 Compressibility	10
3. Experimental Program and Methodology.....	12
3.1 Description of Material and Sample Preparation	12
3.2 Test Methodologies	14
3.2.1 Atterberg Limits tests	14
3.2.2 Lab Vane Testing.....	15
3.2.3 Constant Rate of Strain Test (CRS).....	15
3.2.4 Direct Simple Shear Test (DSS).....	16
4. Results.....	18
4.1 Atterberg Limits	18
4.2 Lab Vane Testing	19
4.3 Constant Rate of Strain Test.....	20
4.4 Direct Simple Shear Test.....	24

5. Synthesis, Analysis and Discussion.....	29
5.1 Atterberg Limits.....	29
5.2 Lab vane test.....	29
5.3 Compressibility.....	30
5.4 Strength.....	34
6. Summary and Conclusions.....	37
7. References.....	38

List of Figures

Figure 1: Types of porosity present in diatomaceous soil, after (Locat et al. 2003).	5
Figure 2: Plasticity chart of literature data. Shaded areas indicate ranges reported for specific soils. Data from Buck Creek, OR (Wang et al. 2021) is shown as blue crosses.	6
Figure 3: Scanning electron microscope (SEM) images of diatoms showing protrusions and indentations (credit; Oregon State University Electron Microscopy Facility).	8
Figure 4: Relationship between strength and percentage of diatomite from undrained direct simple shear tests of mixtures of diatomite and other soils (Wiemer and Kopf (2017)).....	9
Figure 5: Setup of the reconstituting process. (a) Assembly of the Shelby tube, (b) the loading process.....	13
Figure 6: Results confirming the equivalence of the two remolding methods.	14
Figure 7: Plasticity chart comparing the results and data from the literature.	19
Figure 8: Results of the liquid limit from the three testing methods: lab vane, fall cone and Casagrande cup.	19
Figure 9: Stress–void ratio compression curves.	21
Figure 10: Stress-strain compression curves: (a) results from the 4 sites of this research study and (b) a comparison between the results observed and the results reported in the literature.	22
Figure 11: Variation of OCR with consolidation stress.....	23
Figure 12: Typical stress-strain curves observed for diatomaceous silts from all sites and at different OCR = 1,2 and 4.	26
Figure 13: Excess porewater ratio versus shear strain.....	27
Figure 14: Analyzes of the compression index results and empirical correlations.....	31
Figure 15: Analysis of the recompression index results and empirical correlations.	31
Figure 16: Compressibility of the undisturbed and remolded diatomaceous silts.	32
Figure 17: Preconsolidation stress of remolded and undisturbed specimens.	33

Figure 18: Consolidation curves of remolded and undisturbed specimens.33

Figure 19: Graphical determination of SHANSEP parameters.35

Figure 20: Typical variation of strain with (a) normalized vertical stress and (b) normalized excess porewater pressure for undisturbed specimens.....36

List of Tables

Table 1: Classification of diatomaceous soil (Zhang et al. 2013).....	4
Table 2: A summary of LL, PL and PI that has been reported for diatomaceous soils at different sites	6
Table 3: Summary of the basic properties of the diatomaceous soils from the experimental study.....	18
Table 4: Results summary of the constant rate of strain tests.....	21
Table 5: Overconsolidation of the remolded diatomaceous silts.	23
Table 6: Shear strength values for tests from the different test sites.	24
Table 7: Average friction angle from multiple tests of the same specimen.....	28
Table 8: SHANSEP parameters determined for each site.	34
Table 9: Maximum shear stress of remolded and undisturbed W1U9 specimens.	36

1. Introduction

1.1 Background

Diatomaceous soils are sedimentary deposits that are largely composed of diatom microfossils (e.g., Terzaghi et al. 1996). Diatoms are unicellular marine or freshwater algae that have a siliceous, porous exoskeleton (frustule), which is very resistant to weathering due to its symmetrical shape and hard siliceous composition (Antonides 1998; Hamm et al. 2003). The frustules accumulate at the bottom of the water body and are compacted over geological time to form soft, friable, fine-grained siliceous sedimentary rock (Round et al. 1990). Oven-dried samples of diatomaceous earth typically show a preponderance (>80%) of silica (SiO_2) with smaller amounts of alumina, which is attributed mostly to clay minerals, and hematite (Fe_2O_3), among other trace compounds (Antonides 1998). Diatomite deposits form over time from the accretion and compaction of the porous dead diatoms (Antonides 1998). This results in high-porosity, high-moisture content deposits (Shiwakoti et al. 2002; Tanaka and Locat 1999) with distinct physical and mechanical properties in comparison to non-diatomaceous soils (Mesri et al. 1975; Yin 2012). These peculiar sedimentary soils are broadly distributed worldwide, but they are not well-reported in the geotechnical engineering literature. Notably, studies have been reported in the literature on diatomaceous deposits in Japan, China, Colombia, Mexico, and the United States (e.g., Antonides 1998; Day 1995; Díaz-Rodríguez and Santamarina 2001; Hong et al. 2006; Mesri et al. 1975; Wang et al. 2021; Yazdani et al. 2021b). These studies have shown that many of the widely accepted relationships between index properties and strength and deformation behavior of other soils do not apply to diatomaceous soils.

The mechanical behavior of diatomaceous soil is atypical relative to traditional soil mechanics trends. This makes the engineering response of diatomaceous soils difficult to predict without extensive laboratory characterization. As such, more studies are required to develop a comprehensive understanding of the behavior of diatomaceous soils in civil works. Much of

the literature that is available either focuses on mixtures of diatomaceous soil with other soils with well-known engineering properties like kaolinite (e.g., Shiwakoti et al. 2002) or on observations and interpretation of *in-situ* material response (e.g., Wang et al. 2021; Yazdani et al. 2021a). Studies on remolded natural (i.e., not mined or otherwise processed) diatomaceous soil are relatively less common. Most studies on remolded diatomaceous soils are limited mostly to the reporting of consistency limits with relatively little focus on strength and stiffness.

2.1 Research objectives and goals

The limited information available in the literature on engineering properties of diatomaceous soils implies that there are no design methods, either numerical, empirical or analytical, specifically followed when designing on diatomaceous soil. This can be detrimental to the life and serviceability of infrastructure built on diatomaceous deposits. The aim of this research is to assess the engineering behavior of remolded diatomaceous soils from four locations in Oregon: Ady Canal, Moore Park, Pine Cone Drive, and Wikiup Junction. This study includes consistency limit tests, oedometric compression tests, and direct simple shear (DSS) tests to assess the physical and mechanical properties of the diatomaceous soils. The results of this experimental study serve to characterize the fully softened (i.e., critical state) geotechnical properties of diatomaceous soils. Measured results will be compared to those that have been published in the literature. To accomplish the aforementioned goals, the research objectives are as follows:

- i. Comprehensively evaluate the index properties of diatomaceous soil using the fall cone, Casagrande cup, thread rolling, and hand shear vane test methods.
- ii. Study the compressibility of diatomaceous soil using constant rate of strain (CRS) oedometric compression.
- iii. Study the stress-strain-strength behavior of diatomaceous soil through the direct simple shear stress (DSS) test.

- iv. Evaluate the undrained shear strength of the diatomaceous soil using the stress history and normalized soil engineering properties (SHANSEP; (Ladd and Foott 1974a)) procedure from the results of (ii) and (iii).

2. Review of Previous Studies

Diatom microfossils are found in soil deposits where there once was a diatom-bearing waterbody. In its pure form diatomite is white, and other naturally occurring deposits are typically light in color; commonly buff to gray and rarely black, with the overall color being strongly influenced by the non-diatomaceous constituents of the material (Sonyok 2015). In the study of clayey diatomaceous earth deposits in Yunnan, China, Zhang et al. (2013) noted that darker-colored diatomaceous soil possesses more organic materials. Based on the diatom content of the soil, the industrial materials profession has classified diatomaceous soil into five types:

Table 1: Classification of diatomaceous soil (Zhang et al. 2013)

Classification	Description
Pure diatomite	Diatom content is greater than 90%
Clayish diatomite	Diatom content is in the range of 90%-75%
Clayey diatomite or clayey diatomaceous earth	Diatom content is in the range of 75%-50%
Diatomaceous clay	Diatom content is in the range of 50%-25%
Diatomish clay	Diatom content is less than 25%

Frustules have high intraskeletal porosity (Antonides 1998; Franklin 2004; Shiwakoti et al. 2002; Tanaka and Locat 1999). They are symmetrical in shape with complex patterns of nano- to micro-sized pores and open structures resulting in high porosity, low density, and high water affinity (Day 1995; Mesri et al. 1975; Round et al. 1990; Wang et al. 2021). The high porosity is attributed to multiple pore categories that are typically classified into four types, namely: (1) inter-aggregate pores, (2) intra- aggregate pores, (3) skeletal pores, and (4) intra-skeletal pores (Locat et al. 2003; Tanaka and Locat 1999; see Figure 1). The pore spaces that are visible on the surface occupying the chambers making up the microfossil skeleton are skeletal pores,

whereas the interior hollow space is the intra-skeletal pore (Sonyok 2015). The high intraskeletal porosity implies a higher specific surface area for adsorbed water but the silica frustule is chemically inert; thus, the high water content of diatomaceous soils is attributable to capillary action in the intraskeletal pores (Palomino et al. 2011; Wang et al. 2021). These multiple pore families further contribute to diatomaceous soil's affinity for water when compared to non-fossiliferous clays.

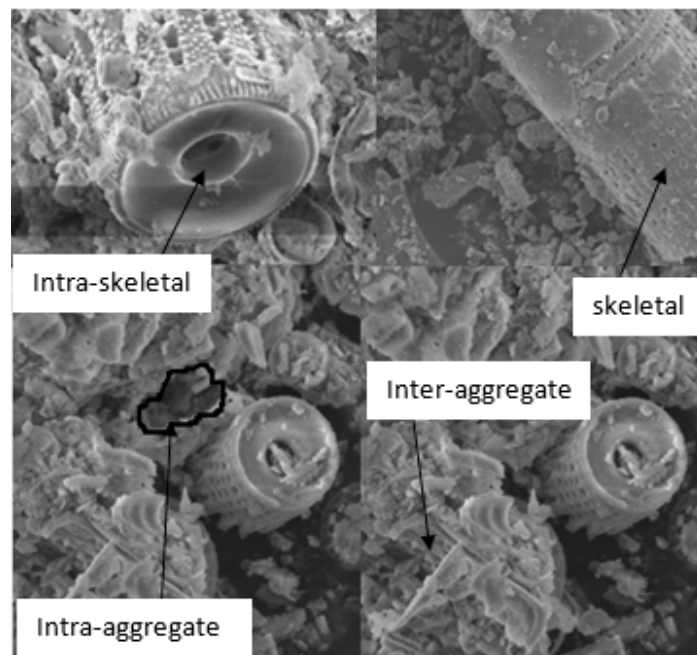


Figure 1: Types of porosity present in diatomaceous soil, after (Locat et al. 2003).

2.1 Atterberg Limits

Diatomaceous soils are typically characterized by high liquid limit (LL) and plastic limit (PL) while the plasticity index (PI) remains relatively unchanged with changing diatom content (Palomino et al. 2011; Tanaka and Locat 1999). As an example, Mexico City clays are reported to have natural water content (w_n), as high as 574% and a PI up to 350 (Díaz-Rodríguez et al. 1998; Mesri et al. 1975). Tanaka and Locat (1999) reported PL, LL and PI in the ranges; 20-45, 79-130 and 10-35 respectively in Osaka Bay clays. A summary of consistency limits reported in the literature is given in Table 2 and is graphically depicted in Figure 2.

Table 2: A summary of LL, PL and PI that has been reported for diatomaceous soils at different sites

Region	LL	PL	PI	Reference
Ariake, Japan	113-157		70-100	Shiwakoti et al. (2002)
Hachirogata, Japan	176-239		110-175	Shiwakoti et al. (2002)
Osaka bay, Japan	79-130	20-45	10-85	Tanaka and Locat (1999)
Buck Creek, Oregon	130-147	70-99	60-48	Wang et al. (2021)
Mexico City, Mexico	11-500	37-150	73-350	Mesri et al. (1975) Diaz-Rodriguez (1998)
Bogotá, Colombia	20-400		10-300	Caicedo et al. (2018)
Mejilones, Chile	73-82		30-38	Ovalle and Arenaldi-Perisic (2021)

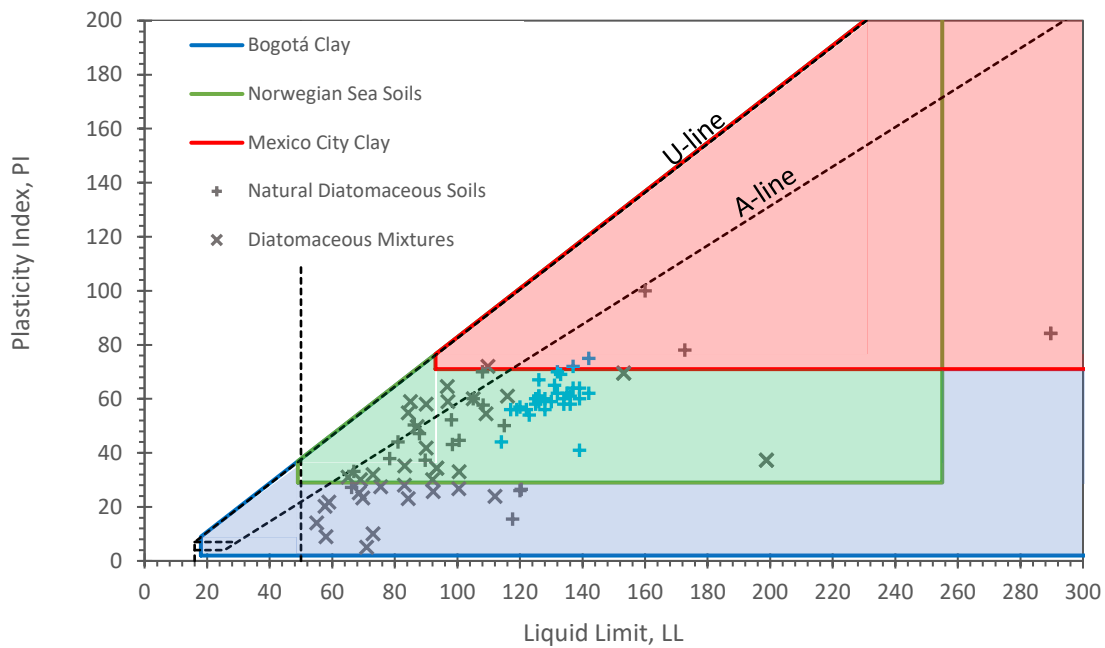


Figure 2: Plasticity chart of literature data. Shaded areas indicate ranges reported for specific soils. Data from Buck Creek, OR (Wang et al. 2021) is shown as blue crosses.

There is an approximate relationship between PI and LL for pure diatomaceous soils but no apparent relationship between PL and LL (Evans and Moug 2020). This can be seen in Bogata clays where the results from consistency limits showed a linear trend between the U-line and the A-line (Caicedo et al. 2018). This behavior of Bogata clays is traditionally observed in high plasticity clays, yet the Bogata clays are very high in quartz ($\approx 50\%$), with feldspars ($\approx 15 - 42\%$), and clay minerals ($\approx 15-30\%$) comprising the remainder of the composition (Caicedo et al. 2018). In contrast, Buck Creek soil does not exhibit a clear linear relationship between LL and PI. The liquid limit of Buck Creek soils varies over a narrow range while the plasticity index is more variable, thus the LL-PI relationship of this soil is more non-linear in comparison to the Bogata clays (Wang et al. 2021).

Due to the wide range in plasticity and inconsistent behavior of diatomaceous soils from various sites/regions, estimating general engineering soil parameters of diatomaceous soils using empirical equations based on index properties has proven difficult (e.g., Hong et al. 2006; Locat and Tanaka 2001; Shiwakoti et al. 2002). The general observation has been that an increase in diatom content results in increased LL and PL. This is attributed to the high water holding capacity of the skeletal and intra-skeletal porosity of diatoms (Locat and Tanaka 2001; Shiwakoti et al. 2002; Tanaka and Locat 1999).

2.2 Shear Strength

Similar to PL and LL, undrained shear strength is reported to increase with an increase in diatom content (e.g., Diaz-Rodríguez 2011). However, unlike the observations made for consistency limits, the shear strength behavior of diatomaceous soil is unlike that of active clays. The shear properties show a strong micro-structural connection which is different from common clays, hence the high shear strengths and internal friction (Shiwakoti et al. 2002; Zhang et al. 2013). The increased strength of diatomaceous soils versus kaolinite is thought to be due to the increase in friction as a result of the rough interlocking surface features of diatom

frustules (Day 1995; Sonyok 2015). These rough surface features are protrusions and indentations of the hollow skeleton of diatoms, as seen in Figure 3.

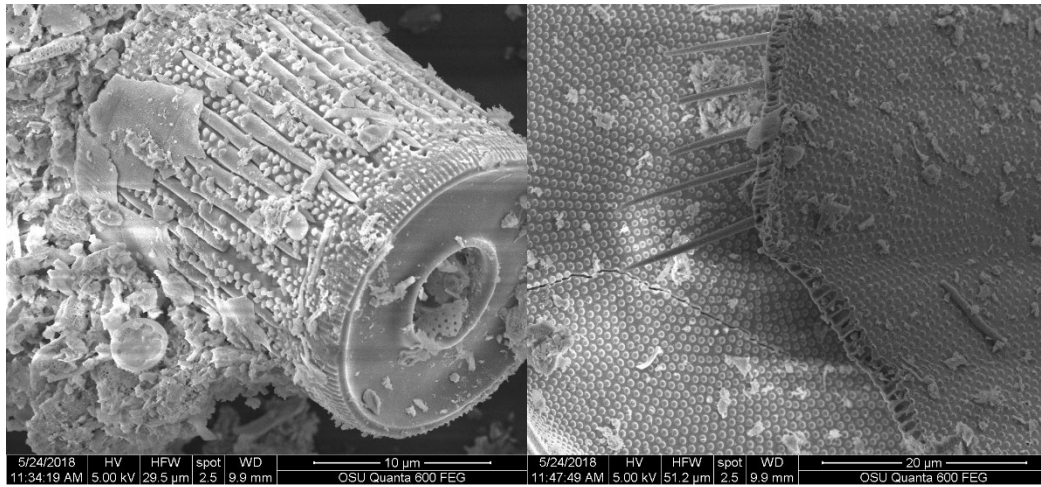


Figure 3: Scanning electron microscope (SEM) images of diatoms showing protrusions and indentations (credit; Oregon State University Electron Microscopy Facility).

Undrained shear strength of $s_u = 44 \text{ kPa}$ and effective stress friction angle of $\phi' = 44^\circ$ were reported for Monterey Formation diatomaceous soils in southern California (Day 1995). Bogota soils in Columbia have a reported shear strength of $\phi' = 35^\circ$ (Caicedo et al. 2018). Similarly, diatomaceous Mexico City clays were observed to have friction angles that vary from 43° to 47° (Díaz-Rodríguez 1992). These high strengths contrast with the typical observation of lower friction angles being associated with higher plasticity. Friction angle has been observed to decrease as PI increases for a variety of non-diatomaceous clay soils (Stark and Member 1994; Xu et al. 2018). Direct shear tests of diatomaceous earth (DE) and clayey-silt (CS) mixtures showed a trend of increasing peak shear strength and friction angle with increasing diatomite content (Wiemer and Kopf 2017). A similar behavior was also observed in diatomite kaolinite mixtures (Díaz-Rodríguez 2011).

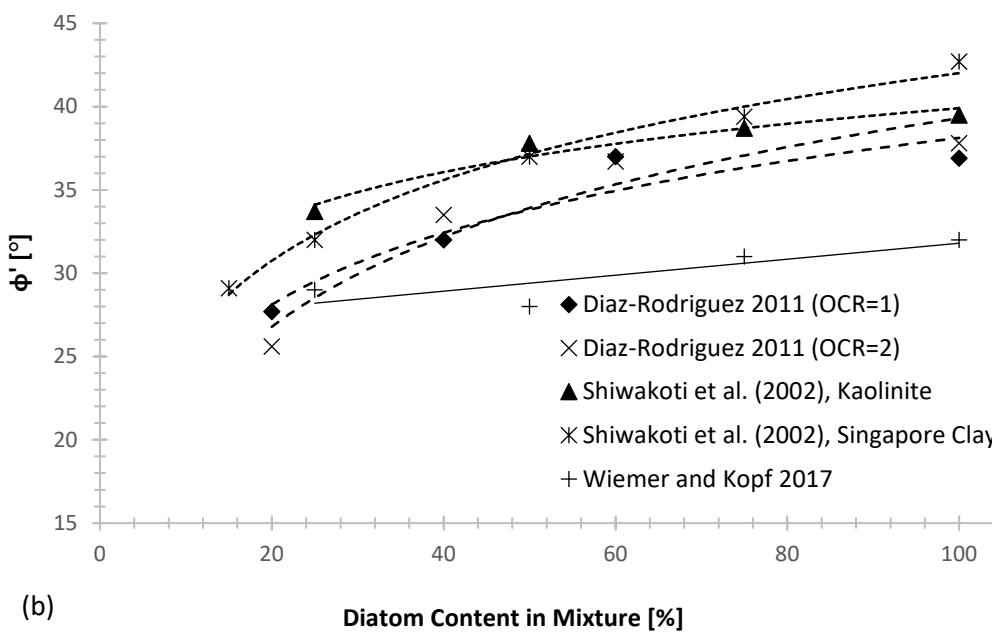
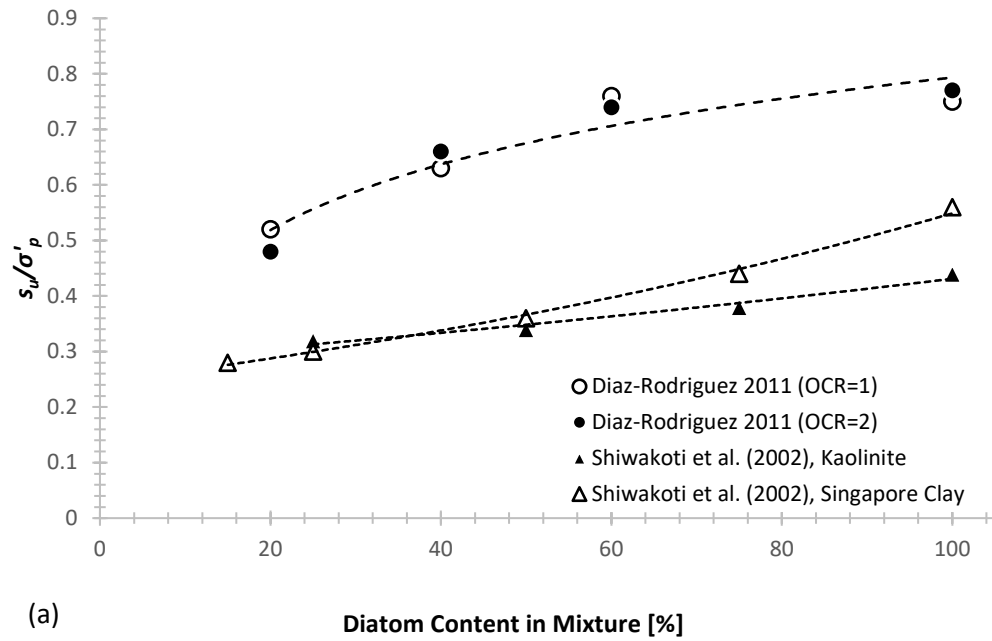


Figure 4: Relationship between strength and percentage of diatomite from undrained direct simple shear tests of mixtures of diatomite and other soils (Wiemer and Kopf (2017))

Shiwakoti et al. (2002) performed direct shear tests of artificial mixtures of diatomite-kaolin, diatomite-Singapore clay and Toyoura sand-kaolin under undrained conditions and observed that dilation properties of the mixtures increased drastically with increasing diatomite content while the stress paths of the Toyoura-kaolin mixture only changed when the content of the sand was 50-75%. These soil mixtures depicted the same behaviors of increasing friction angle with increasing diatom content as reported by (Caicedo et al. 2018; Shiwakoti et al. 2002; Wiemer and Kopf 2017). It can be concluded that diatomaceous soil behaves similarly to sand when it comes to shear strength. However, at high stresses, the friction angle is subsequently lowered due to the crushing of diatoms thus decreasing the overall strength of the soil.

2.3 Compressibility

Compressibility was observed to be relatively low at stresses below 50kPa and it increased as the stress increased (Day 1995). Data on artificial mixtures of diatom and kaolinite by Shiwakoti et al. (2002) showed that because of the hollow structure of diatoms, the addition of diatomite significantly increased the compressibility and coefficient of permeability of the mixtures. Mexico City clay showed a high compression index of 10 (Mesri et al. 1975). This high compressibility has also been observed in natural deposits of diatomaceous soils (Díaz-Rodríguez and González-Rodríguez 2013; Sonyok 2015; Zhang et al. 2013). Tanaka and Locat (1999) also reported compression index, $C_c = 5$ for diatomaceous soils in Japan. The protrusions and perforations of diatoms can explain the higher dilation and compressibility of diatomaceous soils when compared to other similar-sized silica soils (Hong et al. 2006; Sonyok 2015). Diatomaceous soils exhibit broadly non-textbook behavior when their response is measured at the element scale ex-situ (e.g., Sonyok 2015). They have been the cause of excessive post-construction settlement in Wickiup Junction, Oregon and a complex landslide in South-Central Chile (Cornforth Consultants 2017; Wang et al. 2021; Wiemer et al. 2015). This paper seeks to provide depth into the peculiar engineering behavior of diatomaceous soils

by studying the behavior of specimens reconstituted from diatomaceous deposits in Oregon and surrounding areas.

3. Experimental Program and Methodology

3.1 Description of Material and Sample Preparation

Soils tested in this study were collected from four sites: Ady Canal, Moore Park, Pine Cone Drive, and Wickiup Junction. Sampling was done using split spoons and Shelby tubes through mud rotary drilling at Wickiup Junction and hollow stem auger drilling for the other three sites. Both disturbed samples (split spoon) and undisturbed samples (Shelby tube) were retrieved from all four sites. The tested soils in this study are all from the Shelby tube samples. The Shelby tube specimens were first subjected to laboratory mechanical property tests (such as triaxial test, consolidation test, etc.) and then saved to make remolded soil specimens in this study. The specimens are named in the accordance with the acronym of the site and the acronym for Shelby tube sample with its number: W1U# (Wickiup Junction), AC1U# (Ady Canal), MP1U# (Moore Park), PC1U# (Pine Cone Drive).

The remolded specimens were made by drying samples in a 105°C oven for about a week. The dry soil was then ground by hand and sieved through a number 40-sieve. The retained soil was then mixed with deionized water and the resulting slurry was covered and allowed to rest for at least 24 hours before conducting any tests. The slurry from sieved soil was primarily used for conducting Atterberg limits tests.

Modified versions of the slurry consolidation method were adapted for the remolding of specimens (Díaz-Rodríguez and González-Rodríguez 2013; Mesri et al. 1975). The slurry was poured into a 100-mm tall stainless-steel tube with an inner diameter of 72 mm and a wall thickness of 2 mm. The filter paper was placed on each end of the slurry, between the porous stones and slurry to avoid clogging the porous stones. The top porous stone had a diameter small enough to fit into the inner diameter of the tube, thus making it possible to consolidate the specimen by applying load on the top porous stone. The slurry was partially covered with

plastic film to prevent fast drying and allowed to sit for a day or two for it to be stiff enough to carry the load.

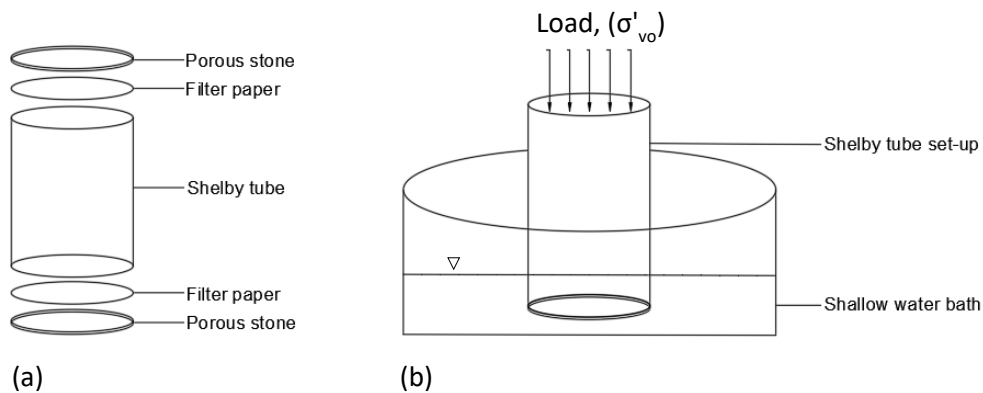


Figure 5: Setup of the reconstituting process. (a) Assembly of the Shelby tube, (b) the loading process.

Initially, incremental dead load was used for specimen consolidation. Once the slurry in the Shelby tube was stiff enough to carry the small weight, a series of loads were placed incrementally on the specimen until the total weight was equivalent to the vertical *in-situ* stress interpreted from cone penetration tests. The total load remained on the specimen for 2-3 weeks to ensure uniform consolidation throughout the Shelby tube. The Shelby tube remained in a shallow pool of deionized water throughout the test to ensure full saturation of the specimens.

Because this procedure was time consuming, a second approach, using a lever arm consolidometer was developed. The same procedure was used for specimen preparation, but at a slightly lower water content because the specimen had to be stiffer before loading. The soil mixture was carefully spooned into an oedometer ring and mounted on the consolidometer. The load was applied to the specimen and deformation was monitored using a potentiometer connected to a digital data acquisition system. Once deformation largely stopped (i.e., when the displacement graph plateaued, indicating the end of primary consolidation), the specimen was considered ready for subsequent testing. To confirm the equivalence of the two approaches, two identical specimens are prepared (one for each method) and the specimens

were subjected to CRS oedometric loading. The results are presented in Figure 6 and indicate that the two specimens behaved equivalently.

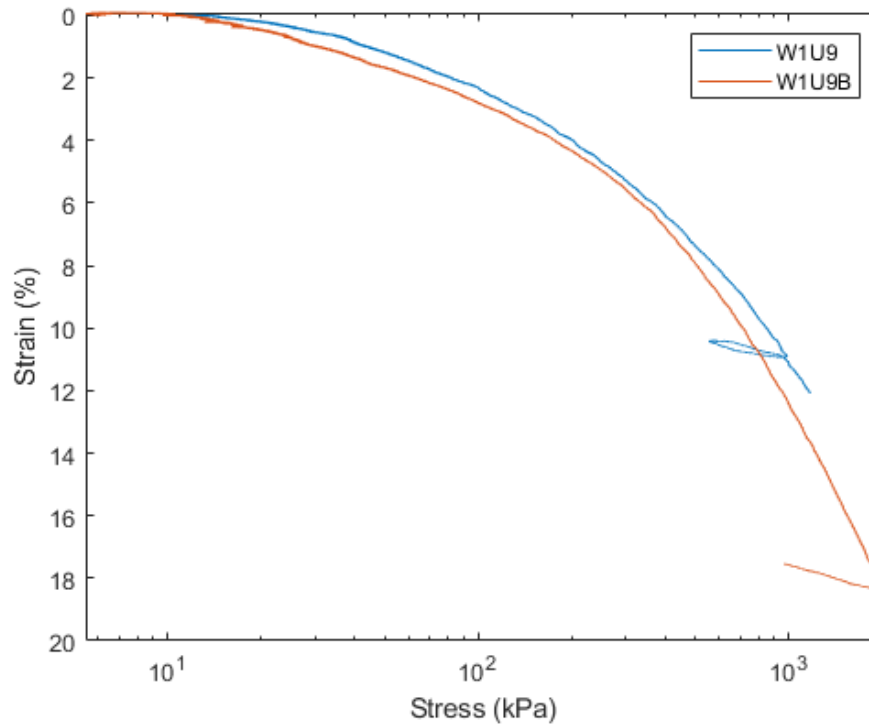


Figure 6: Results confirming the equivalence of the two remolding methods.

3.2 Test Methodologies

3.2.1 Atterberg Limits tests

Liquid limit (LL) and plastic limit (PL) were determined in general accordance with ASTM D4318-17 (2017). Specimens were prepared following Procedure 2 (dry preparation procedure). The multipoint test method (Method A) was used to determine the liquid limit. The standard dictates testing from the driest possible specimen to the wettest; however, in this experimental program, the specimens were first tested from the wettest consistency to the driest and then from the driest to the wettest. Since the slurry was prepared and allowed to stand for 24 hours before testing, it was more convenient to start the tests from the wettest state of the slurry to the least wet. A comparison of results from tests conducted from the least wet state to

the wettest state showed no significant difference. In addition, the liquid limit was also measured following the British Standard BS 1377-2 (1990).

3.2.2 Lab Vane Testing

Laboratory vane shear tests were conducted in general accordance with ASTM D4648 (2016). A SoilSaber hand-held electronic vane shear device was used in the testing, resulting in a direct measurement of the fully-remolded undrained shear strength (s_u) of the soil at very low mean effective stresses. This phase of the work was principally motivated by the difficulties associated with measuring the liquid limit of diatomaceous soil reported in the literature (e.g., (Wang et al. 2021)). It is generally accepted that the undrained shear strength of all soils at their liquid limit is in the range of 1.3-2.4 kPa (e.g., Wood and Wroth 1978; Wroth and Wood 1978), and Wroth and Wood (1978) suggest that 1.7 kPa is the most appropriate value to use. The original work on the development of the fall cone to measure shear strength by Hansbo (1957) implies that soil with a shear strength of 2.0 kPa will allow an 80-g cone with a 30° apex to penetrate 20 mm, which is exactly the definition of LL in BS1377-2 (British Standards Institute 1990). Hence, the vane shear test can provide a robust, theoretically-based check on the liquid limits measured with the Casagrande cup and fall cone test.

3.2.3 Constant Rate of Strain Test (CRS)

Oedometric compression testing was performed following ASTM D4186-20 (2020). The test was performed at strain rates of 5% per hour, under drained conditions following the Method A test procedure. Calculations of the total and effective vertical stresses and vertical strain from the measurement of axial force, axial deformation, and base excess pressure were made. The Casagrande method (e.g., Bardet 1997) was used to determine pre-consolidation stress, σ'_p . The compression index, C_c , and recompression index, C_r were determined from the void ratio-stress ($e - \log \sigma'_v$) curve and, similarly, the strain-stress, ($\gamma - \log \sigma'_v$) curve was used to determine the modified compression index, $C_{c\varepsilon}$, and the modified swell index, $C_{r\varepsilon}$.

3.2.4 Direct Simple Shear Test (DSS)

The direct simple shear tests were performed following ASTM D6528-17 (2017). The shear strength of the remolded specimens was determined in two ways:

- 1) The shear strength was determined at stresses equal to the remolding stress (σ'_{v0}), as discussed in Section 3.1. Specimens were mounted in the device and then reconsolidated to σ'_{v0} before shearing to a maximum shear strain of $\gamma = 25\%$ over 5 hours.
- 2) The specimen was mounted in the device and a vertical effective stress of $\sigma'_v > \sigma'_{v0}$ was applied (in practice, this value was $\sigma'_v = 400 \text{ kPa}$). At the end of primary consolidation, the specimen was either sheared ($OCR = 1$), unloaded to $\sigma'_v = 200 \text{ kPa}$ and sheared ($OCR = 2$) or unloaded to $\sigma'_v = 100 \text{ kPa}$ and sheared ($OCR = 4$).

The results of the DSS test were analyzed using the SHANSEP method (Ladd and Foott 1974a). The SHANSEP procedure estimates the stress history and behavior using the following relationship:

$$\left(\frac{s_u}{\sigma'_v}\right)_{oc} = \left(\frac{s_u}{\sigma'_v}\right)_{nc} OCR^m$$

where s_u = undrained shear strength at a given vertical effective stress, σ'_v ; m = strength increase exponent; and the subscripts 'oc' and 'nc' denote overconsolidated and normally consolidated conditions, respectively. The SHANSEP equation is sometimes expressed as:

$$\left(\frac{s_u}{\sigma'_v}\right)_{oc} = S \cdot OCR^m$$

and S and m are both treated as fitting parameters. However, it can be readily shown through arguments from critical state soil mechanics that, $S = \left(\frac{s_u}{\sigma'_v}\right)_{nc}$ (as originally observed phenomenologically by Ladd and Foott 1974b) and $m = 1 - \frac{c_r}{c_c}$.

4. Results

4.1 Atterberg Limits

From the Atterberg limit tests, compression tests and shear strength, the basic properties of the diatomaceous silts are reported in Table 3

Table 3: Summary of the basic properties of the diatomaceous soils from the experimental study.

Sample ID	G_s	LL	PL	PI
AC1U3	2.5	103	50	53
AC1U5	2.2	112	78	34
AC1U6	2.3	160	107	53
MP1U3	2.2	152	80	72
MP1U9	2.1	122	107	15
PC1U4	2.3	126	60	66
PC1U7	2.1	149	98	51
W1U9	2.4	91	57	34
W1U12	2.2	112	69	43

The results of the Atterberg limits tests are graphically presented in the plasticity chart in Figure 7. The solid symbols represent BS 1377-2 (1990) results and the hollow symbols represent ASTM D4318-17 (2017) results. Most of the soil samples plot below the A-line with LL>50. As such, the soils classify as high-plasticity silts in the Unified Soil Classification System (USCS). The results are largely consistent with the data presented in the literature for other diatomaceous soils (Ovalle and Arenaldi-Perisic 2021; Sonyok 2015; Wiemer and Kopf 2017; Zhang et al. 2013).

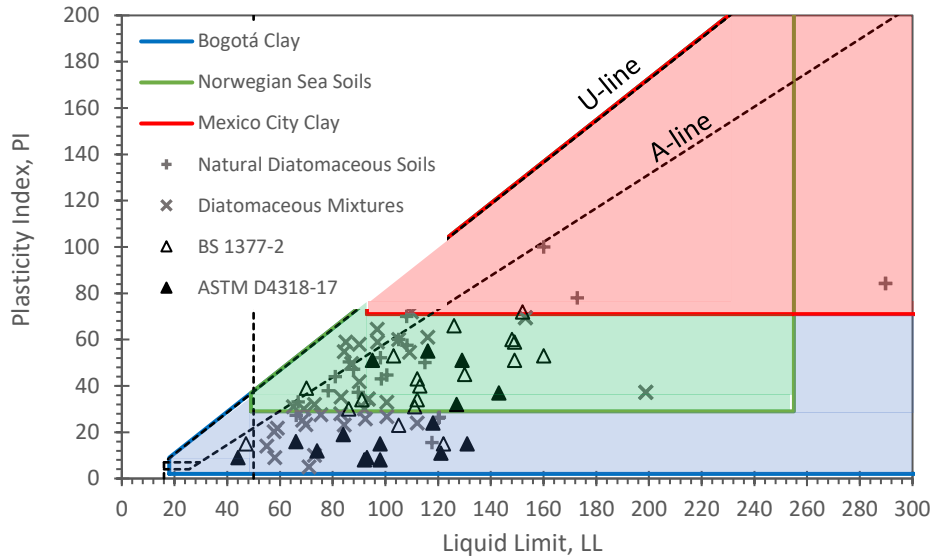


Figure 7: Plasticity chart comparing the results and data from the literature.

4.2 Lab Vane Testing

The lab vane test was conducted to assess the reliability of the results obtained from the *BS 1377-2* (1990) and *ASTM D4318-17* (2017) testing methods. The results shown in Figure 8 indicate that *BS 1377-2* (1990) testing method closely coincides with the lab vane results. The *ASTM D4318-17* (2017) results underestimate the liquid limit when compared with the lab vane results.

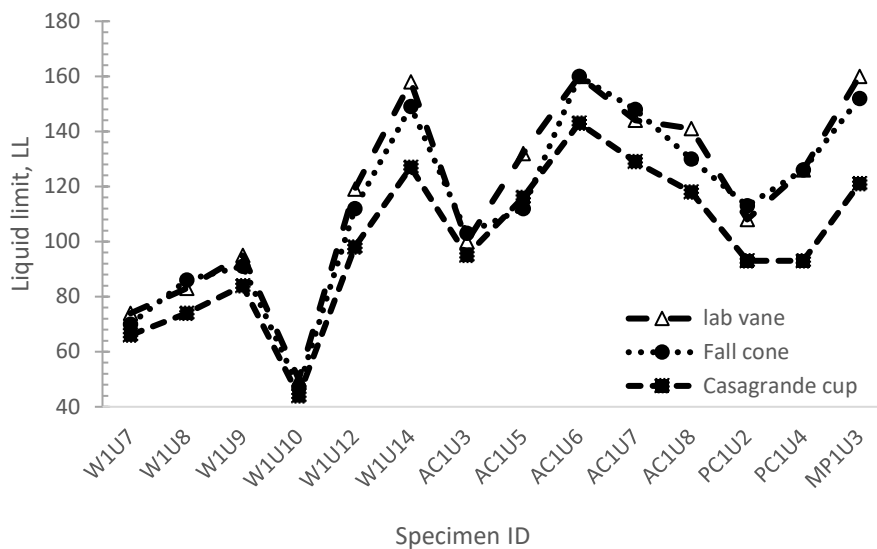


Figure 8: Results of the liquid limit from the three testing methods: lab vane, fall cone and Casagrande cup.

4.3 Constant Rate of Strain Test

CRS tests were performed at a strain rate of 0.003s^{-1} . The specimens were loaded to a vertical effective stress of $\sigma'_v \geq 2000 \text{ kPa}$ and then unloaded long enough to have a clearly defined recompression curve. The results of the CRS test are summarized in Table 4 from $e - \log \sigma'_v$ and $\gamma - \log \sigma'_v$ curves, respectively. The preconsolidation stress was determined graphically by the Casagrande method. The compression index ranges between 0.470 – and 0.897. These compression index values are low when compared to those reported by Tanaka and Locat (1999) which ranged from 1.00 – 4.68. The compression ratio (C_c/C_r) is in the range of 4.92 – 7.73.

The results of the CRS tests are graphically presented in Figure 9 and Figure 10. Figure 9 depicts the relationship between the stress and void ratio. The compression curves do not show a clear break indicating an apparent preconsolidation stress. This is similar to that observed in Mesri et al. (1975) which is a contrast to Tanaka and Locat (1999), who observed a sharp break at the apparent pre-consolidation stress. This can be attributed to the higher stresses observed in their results. Notably, Sonyok (2015) observed that in remolded kaolin-diatom mixtures, the radius of curvature increased when the diatom content was 60% or greater. This trend was reported for stresses similar to those applied in this experimental study. The pre-consolidation stress results from $e - \log \sigma'_v$ (Figure 7) and $\gamma - \log \sigma'_v$ (Figure 8(a)) curves coincide with each other.

Table 4: Results summary of the constant rate of strain tests.

Sample ID	Stress-Void Ratio				Stress-Strain			
	σ_p (kPa)	c_c	c_r	c_r/c_c	σ_p (kPa)	$c_{c\varepsilon}$	$c_{r\varepsilon}$	$c_{r\varepsilon}/c_{c\varepsilon}$
AC1U3	500	0.66	0.14	0.20	511	0.18	0.04	0.20
AC1U5	438	0.80	0.12	0.14	476	0.29	0.04	0.15
AC1U6	125	0.47	-	-	131	0.11	-	-
MP1U9	600	0.58	0.10	0.18	600	0.19	0.03	0.17
PC1U1	552	0.70	0.11	0.16	600	0.22	0.03	0.15
PC1U4	663	0.55	0.09	0.17	700	0.18	0.03	0.16
W1U9	500	0.54	0.06	0.11	509	0.23	0.03	0.12
W1U12	500	0.90	0.12	0.13	500	0.25	0.03	0.13

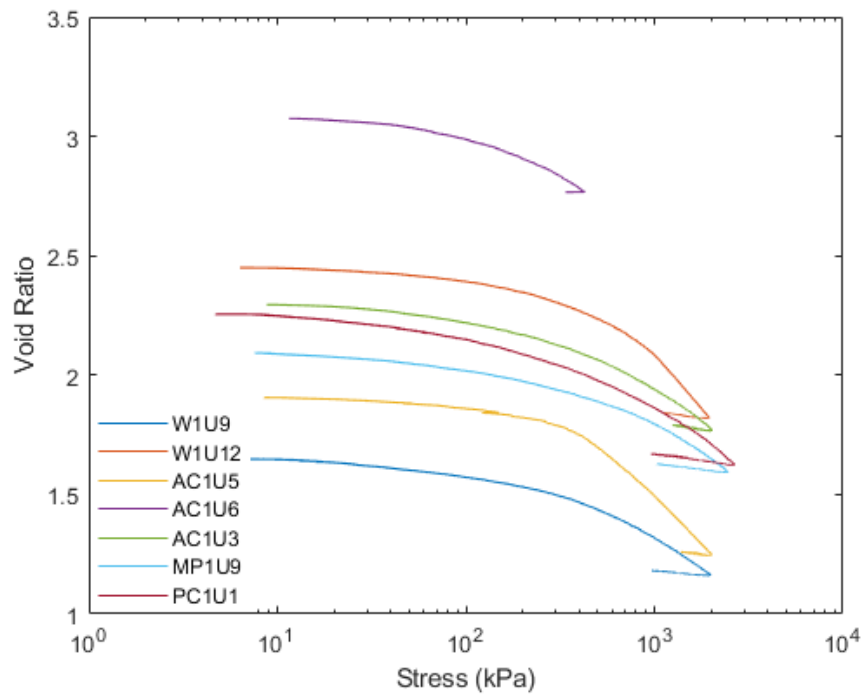


Figure 9: Stress-void ratio compression curves.

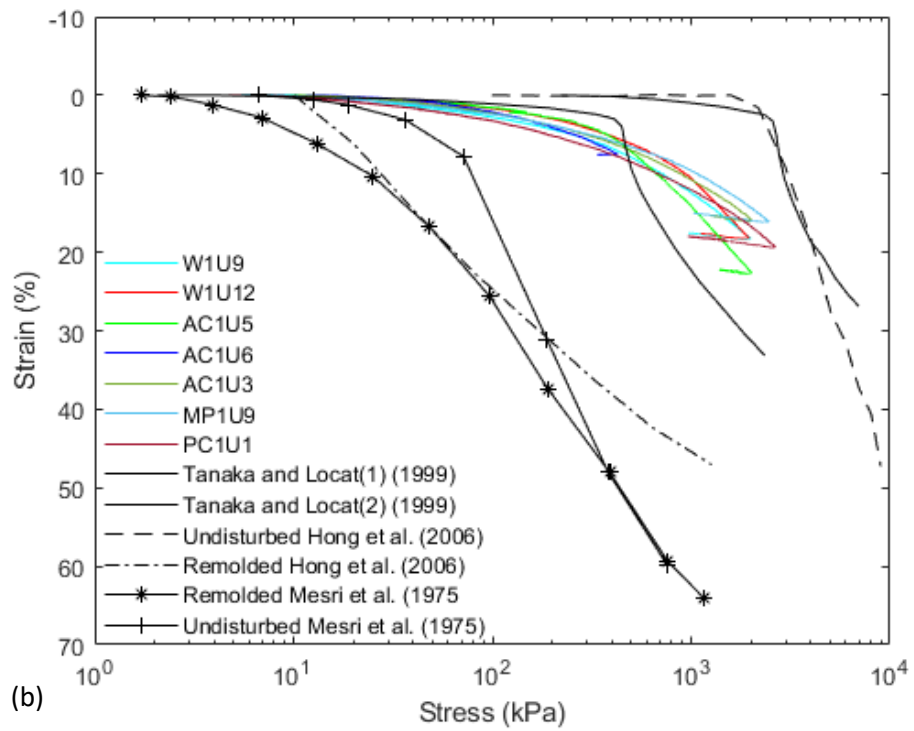
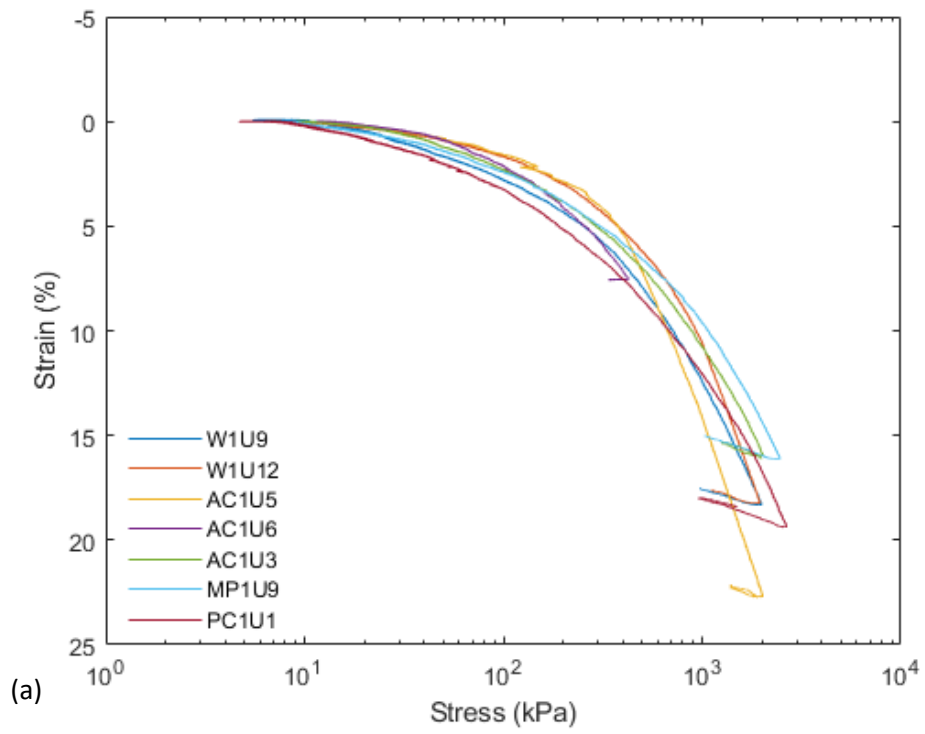


Figure 10: Stress-strain compression curves: (a) results from the 4 sites of this research study and (b) a comparison between the results observed and the results reported in the literature.

An inspection of the overconsolidation ratio for the remolded diatomaceous silts shows that the overconsolidation ratio increased with decreasing consolidation stress. This variation of the overconsolidation ratio with consolidation stress is shown in Figure 11.

Table 5: Overconsolidation of the remolded diatomaceous silts.

Sample ID	σ'_{vo} (kPa)	OCR
AC1U3	118.35	4
AC1U5	146.76	3
AC1U6	154.99	1
MP1U9	132.08	5
PC1U1	32.91	17
PC1U4	57.45	12
W1U9	284.72	2
W1U12	323.72	2

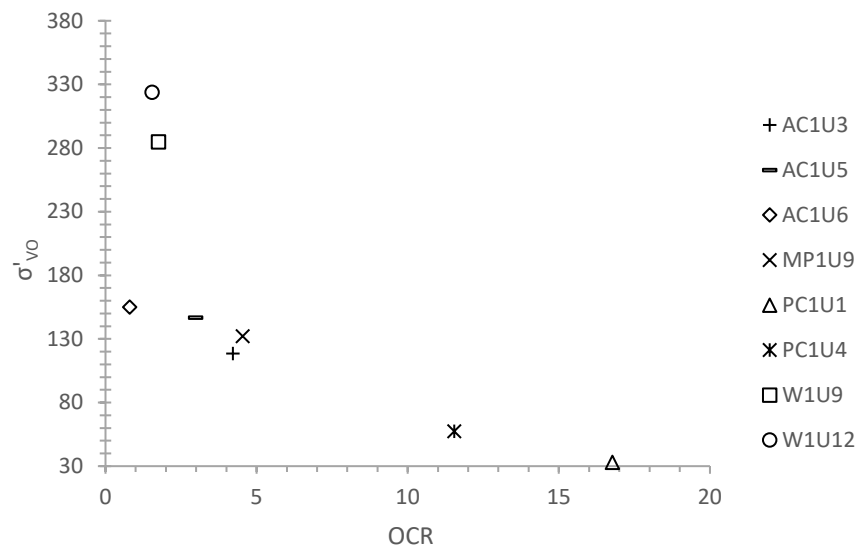


Figure 11: Variation of OCR with consolidation stress.

4.4 Direct Simple Shear Test

In the DSS test scheme, specimens were consolidated to stresses equal to their in-situ or remolding stress. Other specimens were overconsolidated to study the diatomaceous soil's behavior with overconsolidation. Table 6 gives the values of shear strength ($s_u = \tau_{peak}$) and the void ratio determined during each test. For the tests in Table 6, OCR=1. The shear strength is reported as the maximum shear stress attained during the test.

Table 6: Shear strength values for tests from the different test sites.

Sample ID	σ'_{vo} (kPa)	s_u	e
W1U7	255.98	125.40	2.74
W1U9	287.90	126.80	2.06
W1U10	299.00	136.40	2.90
W1U12	323.70	113.80	2.42
AC1U3	118.76	82.40	1.53
AC1U5	146.70	53.10	1.62
AC1U6	155.00	70.70	0.97
AC1U7	163.20	87.80	3.03
MP1U3	100.40	68.20	2.43
MP1U9	132.08	69.90	2.34
PC1U7	82.40	64.70	2.65

The results of the direct simple shear are shown in Figure 12 and Figure 13. In the former figure, typical observations between the normalized shear stress and shear strain for the various samples at the four sites of study. The shear strain-normalized shear stress curves are similar across the four sites. They show a strain hardening phenomenon in nearly all cases. However, it is uncertain whether this is the critical state of the diatomaceous silts since even at the

maximum shear strain of the DSS device (approximately 25%) it was not always evident that a constant stress state had been achieved. The shear strength increases significantly with increasing OCR. Figure 13 illustrates the relationship between shear strain and the normalized excess porewater pressure. These were constant volume tests; therefore, pore water pressure was not measured directly, but was inferred from the changing applied vertical stress required to maintain a constant specimen height. The results indicate the generation of negative excess porewater pressures under high OCR values, consistent with predictions from critical state soil mechanics (e.g., Schofield and Wroth 1968; Wood 1991). The over-consolidated direct simple shear behavior of the diatomaceous silt mimics that of clays under undrained triaxial compression. At lower overconsolidation ratios, positive porewater pressures are induced and as the overconsolidation ratio increases, negative pore water pressures become dominant (Gu et al. 2016).

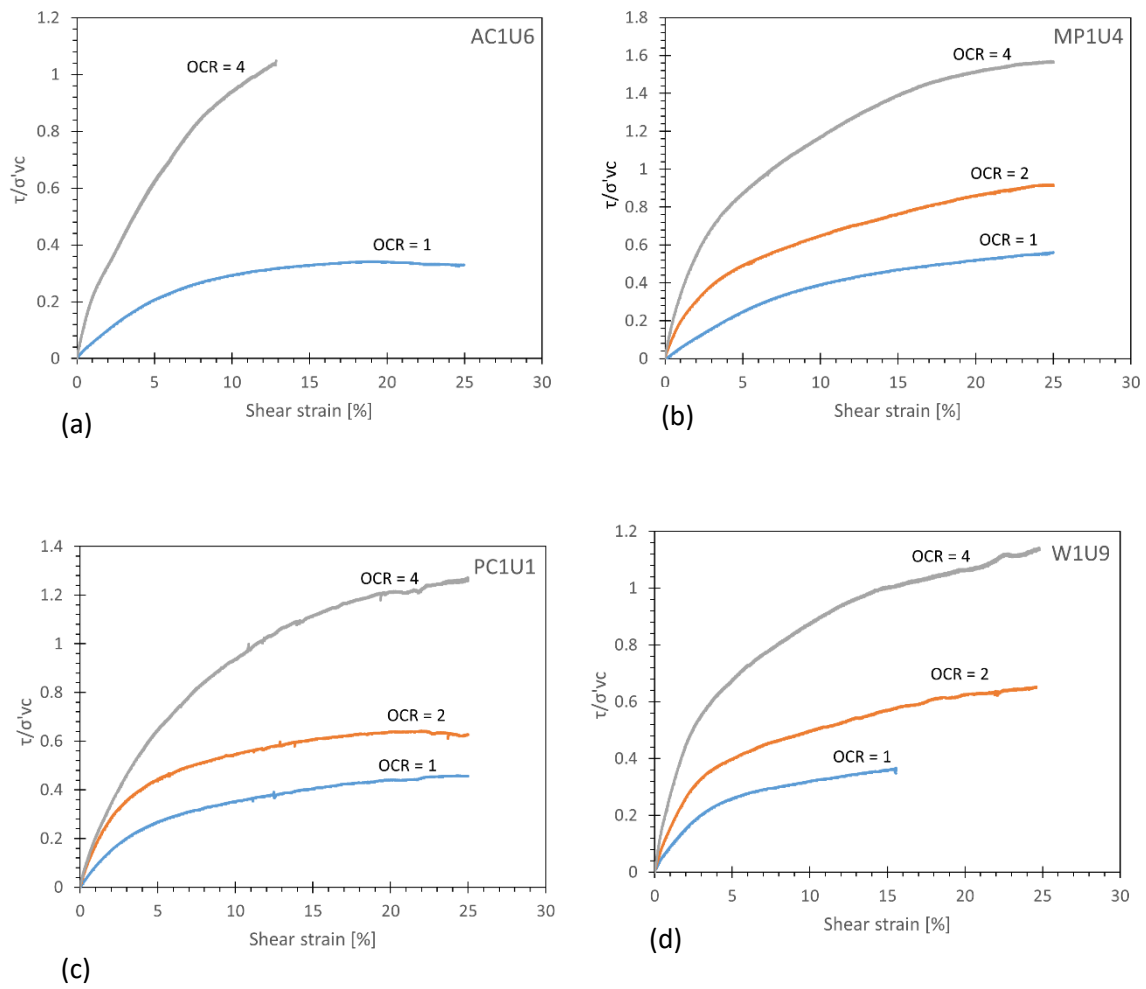


Figure 12: Typical stress-strain curves observed for diatomaceous silts from all sites and at different OCR = 1, 2 and 4.

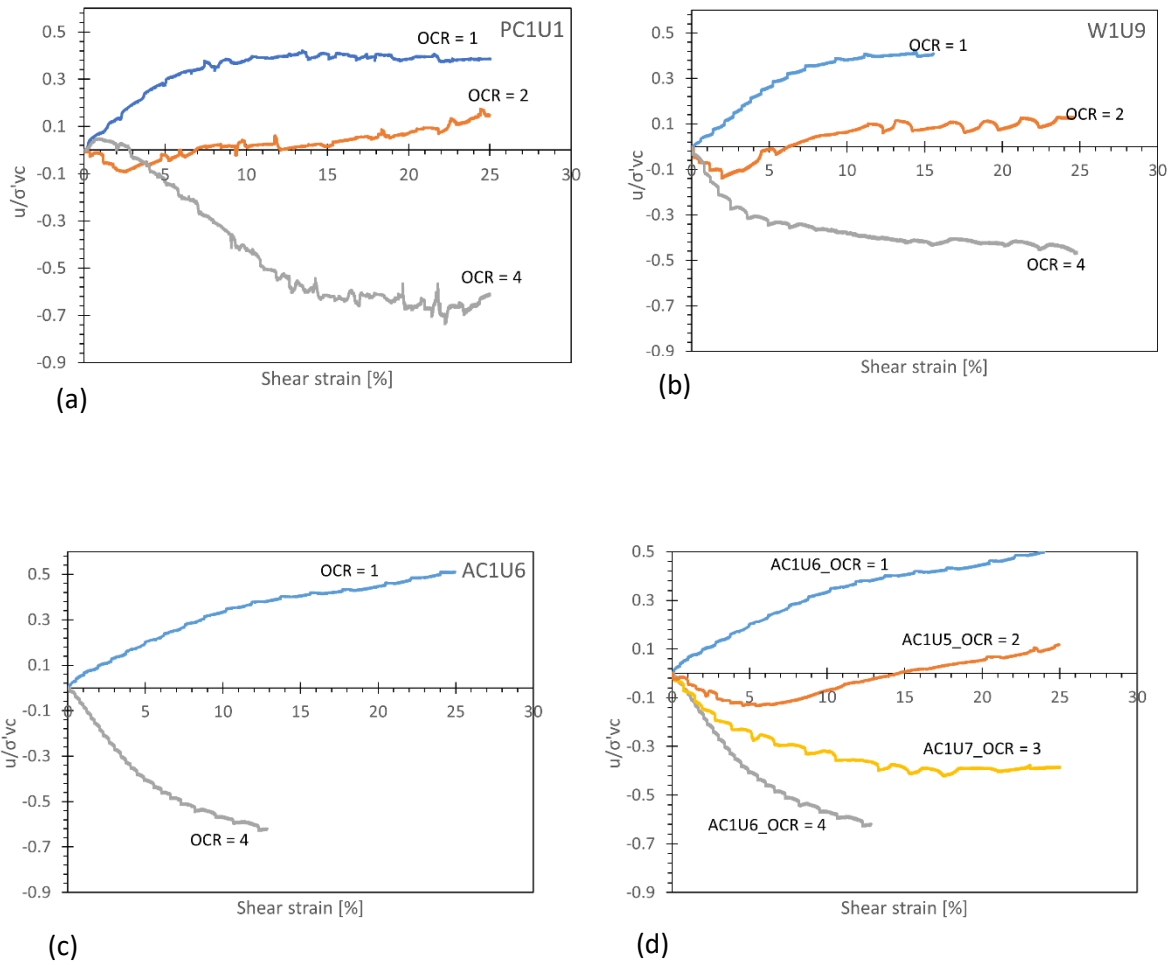


Figure 13: Excess porewater ratio versus shear strain.

Effective stress friction angles (ϕ') were computed from shear stress and vertical effective stress at peak stress. These values imply that the diatomaceous silts have generally high friction angles across three of the four sites, with Moore Park being an exception. The values of the friction angle are presented in Table 7. The expression used for calculating the friction angle is:

$$\phi' = \tan^{-1}\left(\frac{\tau}{\sigma'_{vc}}\right)$$

Table 7: Average friction angle from multiple tests of the same specimen.

Sample ID	ϕ' (degrees)
W1U12	31.70
W1U10	35.90
W1U9	35.03
W1U7	36.75
AC1U6	37.70
AC1U5	32.90
AC1U3	38.20
MP1U9	28.00
PC1U7	38.90

5. Synthesis, Analysis and Discussion

5.1 Atterberg Limits

Atterberg limits are water contents at specified conditions. This means the increased capacity of diatoms to hold water is expected to increase the plasticity indices of diatomaceous silts. However, what is not clear is which proportion of the porewater contributes to the elevated plasticity indices. Of particular interest is whether or not the skeletal and intraskeletal porewater affects the properties of these diatomaceous silts and to what extent.

The increased porosity of diatomaceous soils increases the specific mass of the soils. However, since diatoms are inert, they do not have an adsorbed water layer that can significantly increase the water content. The hypothesis is that the high water holding capacity of diatomaceous silts is caused by capillary action in the intra-skeletal pores. This intra-skeletal pore water is measurable water content that can be evaporated in the oven but does not participate in the particle-particle interactions that are quantified by liquid limit and plastic limit tests. However, at high stresses, the crushing of the frustules can release the skeletal and intraskeletal porewater into the larger particle structure. When the skeletal and intraskeletal porewater is released, it is possible that the consistency limits of the diatomaceous silts at high stresses are not the same as those measured in Atterberg limit tests. This is a possible explanation for the difficult engineering behavior observed in the field that is not readily characterized in the laboratory.

5.2 Lab vane test

The liquid limits derived from the lab vane test showed closer agreement with the measurements from the fall cone tests than from the Casagrande cup measurements. Given the theoretical basis of the lab vane approach, the fall cone test is a preferable method of liquid limit determination for the diatomaceous silts in this study.

5.3 Compressibility

From the CRS tests, the average values of C_c and C_r across all sites are 0.620 and 0.101 respectively. Empirical relationships based on fine-grained plastic soils that relate PI and LL to C_c show opposing compression index values. This difference is shown in Figure 14. The empirical relationship by Terzaghi et al. (1996) is:

$$C_c = 0.009 * (LL - 10).$$

Even though it has been widely used in practice, it is noted to be applicable to normally consolidated clays. The PI correlation is:

$$C_c = PI/74 \text{ (Kulhaway and Mayne 1990).}$$

It is based on the modified Cam clay model using the typical value of specific gravity for clays ($G_s = 2.7$) (Wroth and Wood 1978).

Another relationship that uses the critical state soil mechanics argument states that:

$$C_c = G_s * PI/200 \text{ (Wood 1990).}$$

This relationship makes use of the soil's G_s and it can be observed in Figure 15(a) that it plots closely to Kulhaway and Mayne (1990) results. Regression models based on the natural water content and void ratio were also used to analyze the compressibility of the diatomaceous silts. The equations for these regressions are given below (Azzouz et al. 1976; Elnaggar and Krizek 1971):

$$C_c = 0.40 * (e_o + 0.01 * w_n - 0.025)$$

$$C_r = 0.142 * (e_o - 0.0009 * w_n + 0.006)$$

$$C_r = 0.156 * e_o + 0.01107.$$

These regression lines were formulated from hundreds of compressibility tests and have been found useful for estimating soil's compressibility using soil index properties. Approximations based on critical soil mechanics tend to underestimate the compression index while values based on empirical data overestimate both the compression index and recompression index (Figure 15).

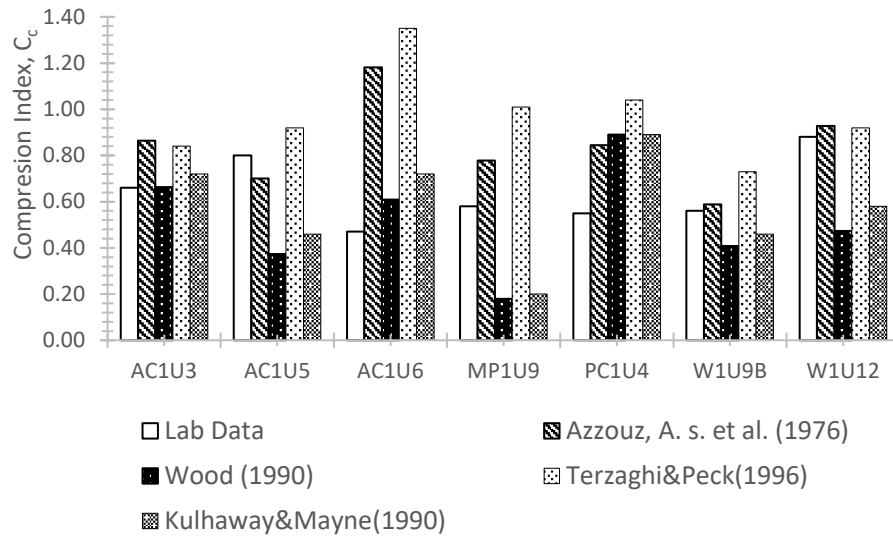


Figure 14: Analyzes of the compression index results and empirical correlations.

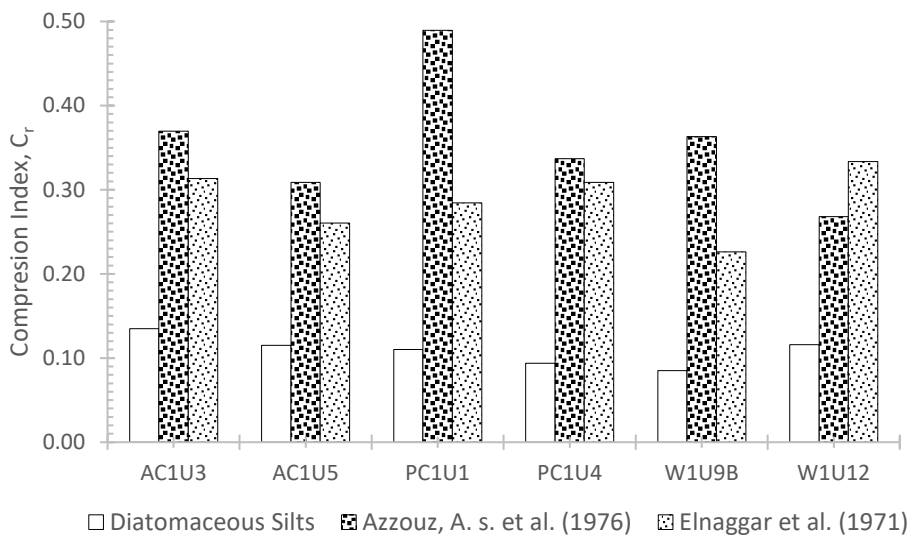


Figure 15: Analysis of the recompression index results and empirical correlations.

A separate study on undisturbed diatomaceous silts from the same sites was conducted. The compressibility of the remolded diatomaceous soils is higher than the compressibility of the undisturbed diatomaceous silts Figure 16. Reworking of the soil breaks down the structure of the frustules and this makes it more susceptible to compression.

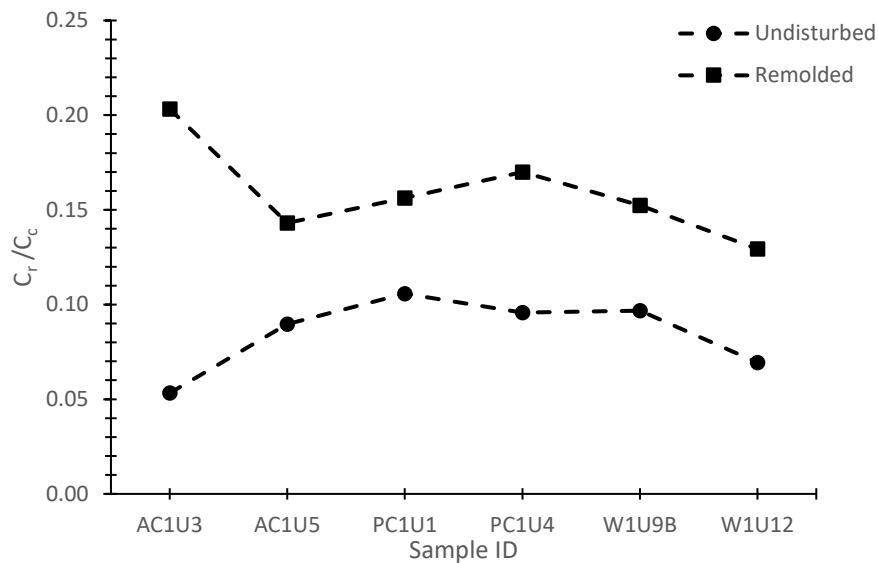


Figure 16: Compressibility of the undisturbed and remolded diatomaceous silts.

The preconsolidation stress of the remolded specimens is more or less the same as that of the undisturbed specimens. On average the preconsolidation stress for the remolded specimens and undisturbed specimens was 485kPa and 526kPa respectively. The consolidation curves of the undisturbed specimens show a clearer break at the point of preconsolidation stress when compared to the remolded soil specimens (Figure 18).

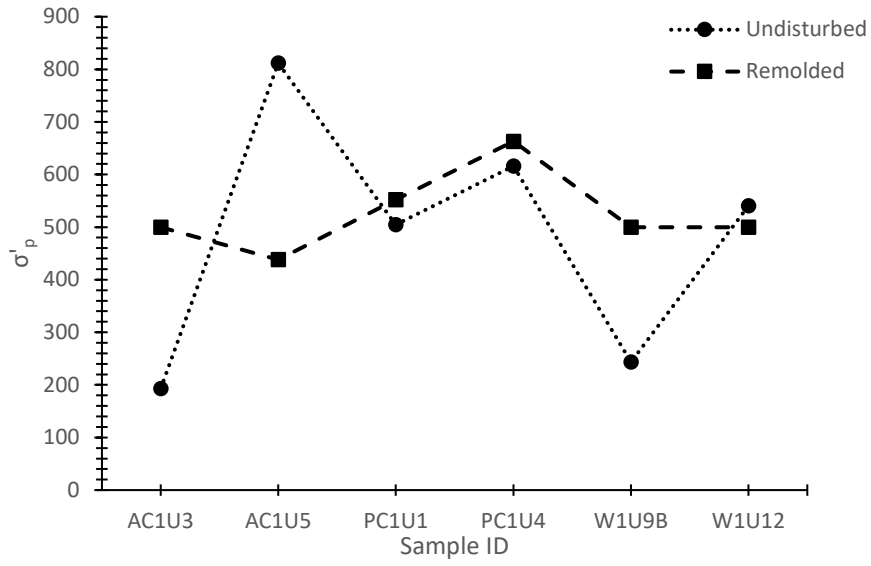


Figure 17: Preconsolidation stress of remolded and undisturbed specimens.

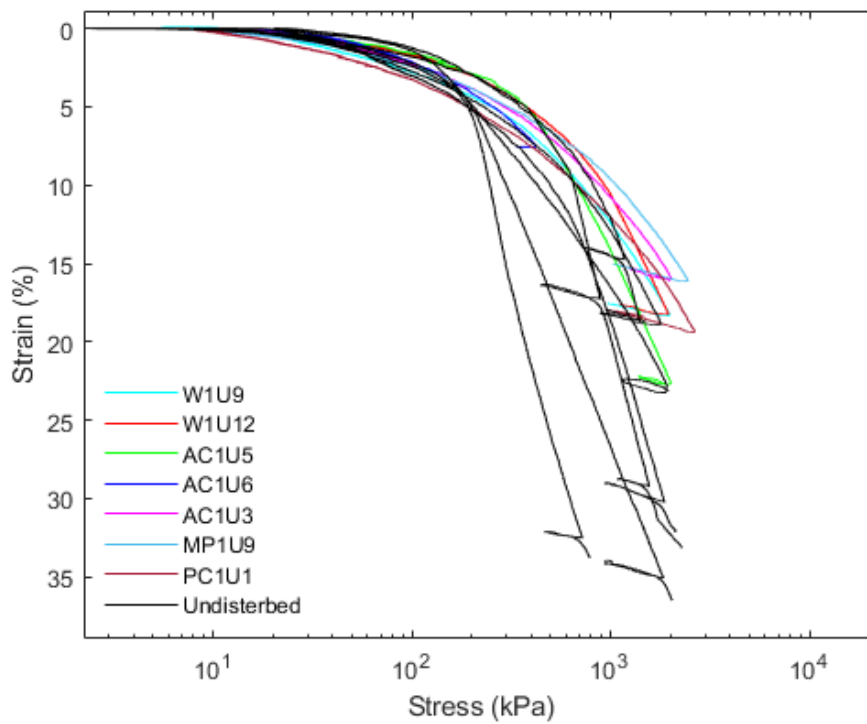


Figure 18: Consolidation curves of remolded and undisturbed specimens.

5.4 Strength

The strength of the diatomaceous silt was analyzed following the SHANSEP procedure as discussed in Section 3.2.4. SHANSEP parameters were derived and are summarized in Table 8. The R^2 denotes the proportion of variance in the variables used to calculate m and S . Ladd (1991) determined m to range from 0.75 to 1 for clays. The results fall within this range. This clay-like behavior can be expected because the diatomaceous silts exhibit properties similar to those of clays. An illustration of the graphical determination of the SHANSEP parameters is given in Figure 19. The strength increase exponent, m is the slope of the linear regression and S is determined from the y-intercept of the power law regression line. The normalized strength value, S is higher than of clays reported in Ladd (1991). This further confirms the findings that diatomaceous soils have an increased strength relative clay as reported in the literature (e.g., Diaz-Rodríguez 2011; Shiwakoti et al. 2002; Wiemer et al. 2015). The m value determined from the SHANSEP procedure was found to be comparable to that derived from the correlation of the compression index and recompression index from the CRS data. Based on the critical state theory, the relationship between the strength increase exponent, compression index and recompression index are as expressed as $m = 1 - C_r/C_c$. The values in Table 8 represent an average from specimens that underwent the CRS test program from each site.

Table 8: SHANSEP parameters determined for each site.

<i>Site ID</i>	<i>m</i>	<i>m</i> $(1 - C_r/C_c)$	<i>S</i>	<i>R</i> ²
Wickiup Junction	0.854	0.851	0.364	0.999
Moore Park	0.861	0.828	0.441	0.996
Pine Cone Drive	0.815	0.840	0.424	0.989
Ady Canal	0.834	0.833	0.319	n/a ¹

¹ Ady Canal had 2 data points only, hence the absence of R^2

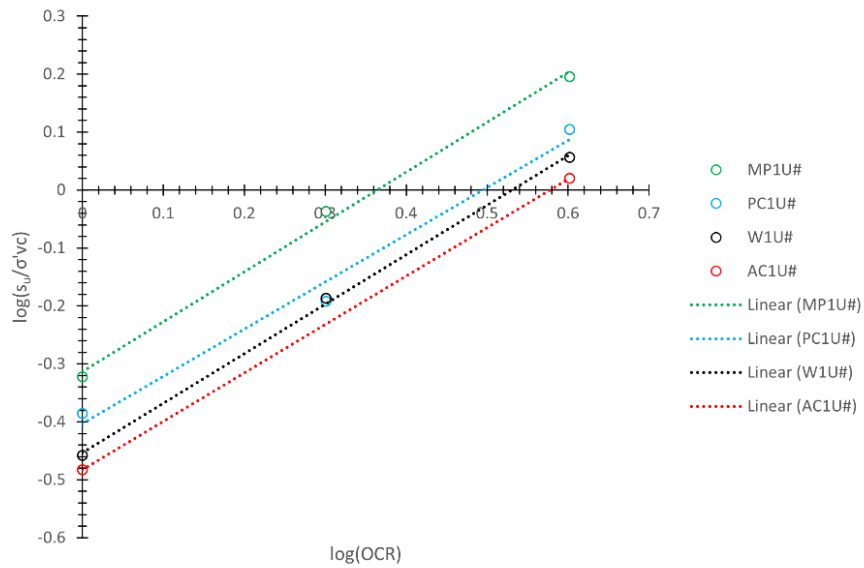


Figure 19: Graphical determination of SHANSEP parameters.

The normalized shear stress and normalized excess porewater behavior of remolded and undisturbed specimens are similar. Figure 20 shows the typical strain-stress and strain-excess porewater performance of the undisturbed samples. The undisturbed specimens depict strain hardening behavior with the most stress attained the highest overconsolidation ratio. Negative excess porewater pressures are induced at higher overconsolidation ratios. These characteristics are the same as those reported in section 4.4 of the results.

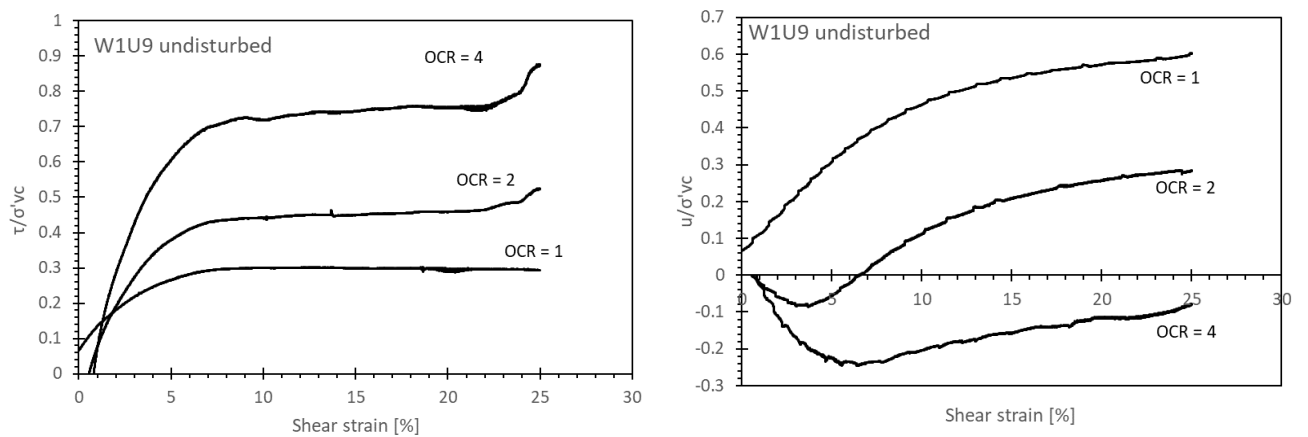


Figure 20: Typical variation of strain with (a) normalized vertical stress and (b) normalized excess porewater pressure for undisturbed specimens.

Both remolded and undisturbed W1U9 specimens were over consolidated to 400kPa and unconsolidated to OCCR =1, 2, and 4. An analysis of the peak shear strength of the various OCRs shows that the remolded W1U9 specimens have higher strength than the undisturbed W1U9 specimens.

Table 9: Maximum shear stress of remolded and undisturbed W1U9 specimens.

OCR	Peak shear stress (kPa)	
	Remolded	Undisturbed
1	147.1	120.7
2	115.6	92.6
3	101	75.1

6. Summary and Conclusions

Diatomaceous silts from Ady Canal, Moore Park, Pine Cone Drive, and Wickiup Junction exhibit properties typical of diatomaceous earth. They have high plasticity properties and relatively high strength. The strength of these diatomaceous silts is improved by the micro-structural connection between the frustules of the diatoms. Based on the results, the following conclusions can be drawn:

- The diatomaceous silts do not conform to the general attribute of fine soils which show decreasing strength with increasing liquid limit. The strength of the diatomaceous is high and the liquid limit is also high.
- Assessment of the liquid limit using fall cone test checks well with the lab vane test determination of the liquid limit.
- Empirical relationships can be used to estimate the compressibility index and recompression index of diatomaceous silts. However, caution should be applied as they tend to either overestimate or underestimate these parameters.
- The compressibility ratio of remolded specimens is higher than of undisturbed specimens.
- Remolded and undisturbed specimens exhibit similar shear behavior under an undrained direct simple shear test at a maximum shear strain of 25%.
- The over consolidated direct simple shear behavior of the diatomaceous silt mimics that of clays under undrained triaxial compression.
- The maximum shear strain attainable in the DSS device (25%) is not high enough to ensure that a critical state has been reached for all specimens.

7. References

- Antonides, L., E. 1998. "Diatomite." *US Geol. Surv. Miner. Commod. Summ.*, 56–57.
- ASTM D3080M-11. 2011. *Test Method for Direct Shear Test of Soils Under Consolidated Drained Conditions*. ASTM International.
- ASTM D4186M-20E1. 2020. *Test Method for One-Dimensional Consolidation Properties of Saturated Cohesive Soils Using Controlled-Strain Loading*. ASTM International.
- ASTM D4318-17. 2017. *Standard Test Methods for Liquid Limit, Plastic Limit, and Plasticity Index of Soils*. ASTM International.
- ASTM D4648M-16. 2016. *Test Method for Laboratory Miniature Vane Shear Test for Saturated Fine-Grained Clayey Soil*. ASTM International.
- ASTM D6528-17. 2017. *Test Method for Consolidated Undrained Direct Simple Shear Testing of Cohesive Soils*. ASTM International.
- Azzouz, A. S., R. J. Krizek, and R. B. Corotis. 1976. "Regression Analysis of Soil Compressibility." *Soils Found.*, 16 (2): 19–29. https://doi.org/10.3208/sandf1972.16.2_19.
- Bardet, J. P. 1997. *Experimental soil mechanics*. Upper Saddle River, N.J: Prentice Hall.
- BS 1377-2 Methods of test for soils for civil engineering purposes: Classification Tests*. 1990. British Standards Institute.
- Caicedo, B., C. Mendoza, F. López, and A. Lizcano. 2018. "Behavior of diatomaceous soil in lacustrine deposits of Bogotá, Colombia." *J. Rock Mech. Geotech. Eng.*, 10 (2): 367–379. <https://doi.org/10.1016/j.jrmge.2017.10.005>.
- Cornforth Consultants. 2017. *Preliminary feasibility study: US 97 at Wickiup junction, La pine, Oregon*. Cornforth Consultants.
- Day, R. W. 1995. "Engineering Properties of Diatomaceous Fill." *J. Geotech. Eng.*, 121 (12): 3.
- Diaz-Rodríguez, A., J. 2011. "Diatomaceous soils: monotonic behavior." Unpublished. <https://doi.org/10.13140/2.1.3322.5606>.

- Díaz-Rodríguez, A., J. 2011. “Diatomaceous soils: monotonic behavior.”
- Díaz-Rodríguez, J. A. 1992. “Yielding of Mexico City Clay and Other Natural Clays.” 118 (7): 981–995.
- Díaz-Rodríguez, J. A., R. L.-S. Cruz, V. M. Dávila-Alcocer, E. Vallejo, and P. Girón. 1998. “Physical, chemical, and mineralogical properties of Mexico City sediments: a geotechnical perspective.” 35: 11.
- Díaz-Rodríguez, J. A., and R. González-Rodríguez. 2013. “Influence of diatom microfossils on soil compressibility Influence des microfossiles de diatomées sur la compressibilité des.” *Proc 18th Int Conf Soil Mech Geotech Eng*, 325–328. French Society for Soil Mech. and Geotech. Engineering.
- Díaz-Rodríguez, J. A., and J. C. Santamarina. 2001. “Mexico City Soil Behavior at Different Strains: Observations and Physical Interpretation.” *J. Geotech. Geoenvironmental Eng.*, 127 (9): 783–789. [https://doi.org/10.1061/\(ASCE\)1090-0241\(2001\)127:9\(783\)](https://doi.org/10.1061/(ASCE)1090-0241(2001)127:9(783)).
- Elnaggar, H. A., and R. J. Krizek. 1971. “Statistical Approximation for Consolidation Settlement.” 10.
- Evans, M., T., and D. Moug. 2020. “Diatomaceous soils: a less than cromulent engineering material.” *Geotech. Sustain. Infrastruct. Dev.*, Lecture Notes in Civil Engineering, P. Duc Long and N. T. Dung, eds., 709–716. Singapore: Springer Singapore.
- Franklin, D. 2004. “Gas Guzzlers.” February 2004.
- Gu, C., J. Wang, Y. Cai, L. Sun, P. Wang, and Q. Dong. 2016. “Deformation characteristics of overconsolidated clay sheared under constant and variable confining pressure.” *Soils Found.*, 56 (3): 427–439. <https://doi.org/10.1016/j.sandf.2016.04.009>.
- Hamm, C. E., R. Merkel, O. Springer, P. Jurkojc, C. Maier, K. Prechtel, and V. Smetacek. 2003. “Architecture and material properties of diatom shells provide effective mechanical protection.” *Nature*, 421 (6925): 841–843. <https://doi.org/10.1038/nature01416>.

- Hong, Z., Y. Tateishi, and J. Han. 2006. “Experimental Study of Macro- and Microbehavior of Natural Diatomite.” *J. Geotech. Geoenvironmental Eng.*, 132 (5): 603–610.
[https://doi.org/10.1061/\(ASCE\)1090-0241\(2006\)132:5\(603\)](https://doi.org/10.1061/(ASCE)1090-0241(2006)132:5(603)).
- Kulhaway, F. H., and P. W. Mayne. 1990. *Manual on Estimating Soil Properties for Foundation Design*.
- Ladd, C. C. 1991. “Stability Evaluation during Staged Construction.” *J. Geotech. Eng.*, 117 (4): 540–615. [https://doi.org/10.1061/\(ASCE\)0733-9410\(1991\)117:4\(540\)](https://doi.org/10.1061/(ASCE)0733-9410(1991)117:4(540)).
- Ladd, C. C., and R. Foott. 1974a. “New design procedure for stability of soft clays.” *J. Geotech. Eng. Div.*, 100 (7): 763–786.
- Ladd, C. C., and R. Foott. 1974b. “New Design Procedure for Stability of Soft Clays.” *J. Geotech. Eng. Div.*, 100 (7): 763–786.
- Locat, J., and H. Tanaka. 2001. “A New Class of Soils: Fossiliferous Soils? Une Nouvelle Classe de Sols: les Sols Fossilifères?” 7.
- Locat, J., H. Tanaka, T. Tan S., G. Dasari R., and H. Lee. 2003. *Characterisation and Engineering Properties of Natural Soils*. CRC Press.
- Mesri, G., A. Rokhsar, and B. F. Bohor. 1975. “Composition and compressibility of typical samples of Mexico City clay.” 28.
- Ovalle, C., and G. Arenaldi-Perisic. 2021. “Mechanical behaviour of undisturbed diatomaceous soil.” *Mar. Georesources Geotechnol.*, 39 (5): 623–630.
<https://doi.org/10.1080/1064119X.2020.1720049>.
- Palomino, A. M., S. Kim, A. Summitt, and D. Fratta. 2011. “Impact of diatoms on fabric and chemical stability of diatom–kaolin mixtures.” *Appl. Clay Sci.*, 51 (3): 287–294.
<https://doi.org/10.1016/j.clay.2010.12.002>.
- Round, F. E., R. M. Crawford, and D. G. Mann. 1990. “The Diatoms: Biology and Morphology of the Genera.” *Camb. Univ. Press*, 10.

- Schofield, A. N., and C. P. Wroth. 1968. *Critical State Soil Mechanics*. European civil engineering series. New York, NY: McGraw-Hill.
- Shiwakoti, D. R., H. Tanaka, M. Tanaka, and J. Locat. 2002. "Influences of Diatom Microfossils on Engineering Properties of Soils." *Soils Found.*, 42 (3): 1–17.
https://doi.org/10.3208/sandf.42.3_1.
- Sonyok, D. R. 2015. "Effect of diatoms on index properties, compressibility, suction, and stiffness of diatomite-kaolin mixtures." *ProQuest Diss. Theses*. Ph.D. United States -- New Mexico: New Mexico State University.
- Standard Test Methods for Liquid Limit, Plastic Limit, and Plasticity Index of Soils*. 2017. ASTM International.
- Stark, T. D., and A. Member. 1994. "Drained Residual Strength of Cohesive Soils." *J. Geotech. Eng.*, 16.
- Tanaka, H., and J. Locat. 1999. "A microstructural investigation of Osaka Bay clay: the impact of microfossils on its mechanical behaviour." 36: 16.
- Terzaghi, K., R. B. Peck, and G. Mesri. 1996. *Soil mechanics in engineering practice*. New York: Wiley.
- Test Method for Consolidated Undrained Direct Simple Shear Testing of Cohesive Soils*. 2017. ASTM International.
- Test Method for One-Dimensional Consolidation Properties of Saturated Cohesive Soils Using Controlled-Strain Loading*. 2018. ASTM International.
- Wang, J., E. Yazdani, and T. M. Evans. 2021. "Case study of a driven pile foundation in diatomaceous soil. I: Site characterization and engineering properties." *J. Rock Mech. Geotech. Eng.*, 13 (2): 431–445. <https://doi.org/10.1016/j.jrmge.2020.10.006>.

- Wiemer, G., and A. Kopf. 2017. "Influence of diatom microfossils on sediment shear strength and slope stability." *Geochem. Geophys. Geosystems*, 18 (1): 333–345.
<https://doi.org/10.1002/2016GC006568>.
- Wiemer, G., J. Moernaut, N. Stark, P. Kempf, M. De Batist, M. Pino, R. Urrutia, B. L. de Guevara, M. Strasser, and A. Kopf. 2015. "The role of sediment composition and behavior under dynamic loading conditions on slope failure initiation: a study of a subaqueous landslide in earthquake-prone South-Central Chile." *Int. J. Earth Sci.*, 104 (5): 1439–1457.
<https://doi.org/10.1007/s00531-015-1144-8>.
- Wood, D. M. 1991. *Soil Behaviour and Critical State Soil Mechanics*. Cambridge: Cambridge University Press.
- Wood, D., Muir. 1990. *Critical State Soil Mechanics*. Cambridge University Press.
- Wroth, C. P., and D. M. Wood. 1978. "The correlation of index properties with some basic engineering properties of soils." *Can. Geotech. J.*, 15 (2): 137–145.
<https://doi.org/10.1139/t78-014>.
- Xu, C., X. Wang, X. Lu, F. Dai, and S. Jiao. 2018. "Experimental study of residual strength and the index of shear strength characteristics of clay soil." *Eng. Geol.*, 233: 183–190.
<https://doi.org/10.1016/j.enggeo.2017.12.004>.
- Yazdani, E., J. Wang, and T. M. Evans. 2021a. "Case study of a driven pile foundation in diatomaceous soil. II: Pile installation, dynamic analysis, and pore pressure generation." *J. Rock Mech. Geotech. Eng.*, 13 (3): 11. Elsevier.
<https://doi.org/10.1016/j.jrmge.2020.10.005>.
- Yazdani, E., J. Wang, and T. M. Evans. 2021b. "Case study of a driven pile foundation in diatomaceous soil. II: Pile installation, dynamic analysis, and pore pressure generation." *J. Rock Mech. Geotech. Eng.*, 13 (2): 446–456. <https://doi.org/10.1016/j.jrmge.2020.10.005>.

Yin, J. 2012. “Mechanical Behavior of Reconstituted Clay Samples Prepared by Large Diameter Oedometer.” *Civ. Eng. Urban Plan.* 2012, 362–368. Yantai, China: American Society of Civil Engineers.

Zhang, Y., C. Guo, X. Yao, Y. Qu, and N. Zhou. 2013. “Engineering geological characterization of clayey diatomaceous earth deposits encountered in highway projects in the Tengchong region, Yunnan, China.” *Eng. Geol.*, 167: 95–104.

<https://doi.org/10.1016/j.enggeo.2013.10.009>.